Design, Test and Analysis of a Gyrotron Cavity Mock-Up Cooled Using Mini Channels

Design, Test and Analysis of a Gyrotron Cavity Mock-up cooled using Mini-Channels

A. Bertinetti, F. Albajar, F. Cau, A Leggieri, F. Legrand, E. Perial, G. Ritz, L. Savoldi, *Member, IEEE*, R. Zanino, *Senior Member, IEEE*, A. Zappatore

***Abstract*— In 2016, we have designed, built and finally tested at the FE200 facility in Le Creusot (France) a planar mock-up mimicking the water-cooled cylindrical resonance cavity of the European 170 GHz, 1 MW gyrotron to be used for electron cyclotron plasma heating in ITER. The aim of the mock-up is the characterization of the cooling capability of the cavity. A Glidcop® target is heated with an electron beam gun with resulting peak heat fluxes relevant for the full-size cavity. Underneath the target surface, whose temperature is monitored by means of a pyrometer, a set of parallel semi-circular mini-channels, with diameter of 1.5 mm, allows the flow of pressurized water, entering the mock-up at ~ 9 bar and 40 °C. Several thermocouples measure the target temperature, at different distances from the heated target surface.**

The experimental results show that the mock-up is capable to withstand a heat fluxes of 21 MW/m^2, while the cooling system keeps the heated surface below ~ 400 °C, for flow conditions comparable to those of the full-size cavity. The test results are used to first calibrate the uncertain model parameters and then, with frozen parameters, to validate a previously developed CFD model, showing good agreement with the experiment. In view of its reliability, this model might eventually be a useful tool for the simulation of the full-size gyrotron cavity operation.

***Index Terms*— CFD, boiling, gyrotron cavity mock-up**

I. Introduction

Plasma heating and current drive in tokamaks can be obtained injecting high power electromagnetic waves into the plasma at the Electron Cyclotron frequency. ITER will adopt gyrotrons in its heating and current drive system [1], which convert the rotational kinetic energy of electrons in microwave energy in a resonator, called "cavity", see Fig. 1.

In the European 170 GHz, 1 MW gyrotron for ITER [2], the cavity is a hollow cylinder (with a diameter of few cm and a thickness of few mm) made of Glidcop® (a copper based alloy) which can nominally withstand high operating temperatures and thermal cycles. The cooling enhancement of the water-cooled cavity, where the peak heat load can reach 20+ MW/m^2 on a very short (~ 1 cm) region, is currently based on the Raschig Rings technology [3]. As an alternative to that, mini-channels (MCs) drilled in a Glidcop® annulus have been proposed, based also on Computational Fluid Dynamics (CFD) preliminary analysis, which demonstrated that this solution could reach higher cooling performance thanks to the high Reynolds number mainly due to the high fluid speed in the channels [4]. After the optimization of the MC layout, to account for the manufacturing and test constraints, in 2016, we have designed and built a planar mock-up, with the aim of assessing the cooling capability of the MC cooling option. The mock-up was eventually tested at the FE200 facility in Le Creusot (France), monitoring of the heated surface temperature as a function of the cooling mass flow rate and heat load. (Note that the flat geometry was adopted, in hydrodynamic similarity with the full-size cavity, to be compatible with the facility constraints, see below).

In this paper, the mock-up design is presented, and the hydraulic similarity with the full-size cavity hidden behind its design is shown. The results of the measurements are summarized and discussed. Then the computed results, obtained using the commercial software STAR-CCM+ [5], are presented.

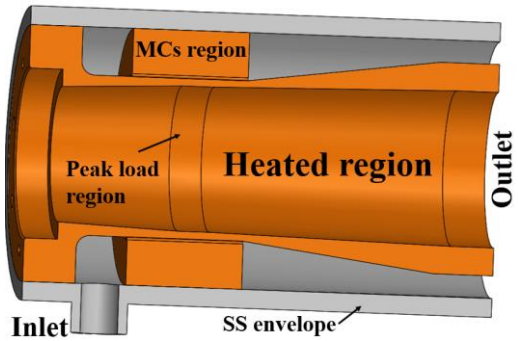

Fig. 1. Schematic view of the inner part of the full-size gyrotron cavity (resonator in orange) in a stainless steel envelope, for the European 170 GHz, 1 MW gyrotron for ITER. The inner diameter of the cavity is ~ 2 cm.

The work leading to this publication has been funded partially by Fusion for Energy under F4E-2015-EXP-223. This publication reflects the views only of the author, and Fusion for Energy cannot be held responsible for any use which may be made of the information contained therein.

A. Bertinetti (andrea.bertinetti@polito.it), L. Savoldi (laura.savoldi@polito.it), R. Zanino (roberto.zanino@polito.it) and A. Zappatore (andrea.zappatore@polito.it) are with NEMO group, Dipartimento Energia, Politecnico di Torino, Corso Duca degli Abruzzi 24, 10129 Torino, Italy

F. Albajar (Ferran.Albajar@f4e.europa.eu) and F. Cau (Francesca.Cau@f4e.europa.eu) are with Fusion for Energy, c/ Josep Pla 2, 08019 Barcelona, Spain

A. Leggieri (alberto.leggieri@thalesgroup.com), F. Legrand (francois.legrand@thalesgroup.com) and E. Perial (etienne.perial@thalesgroup.com) are with Thales Electron Devices, Rue Marcel Dassault 2, 78140 Vélizy-Villacoublay, France

G. Ritz (guillaume.ritz@areva.com) is with Areva NP, 30 Bd de l'Industrie, 71205 Le Creusot, France

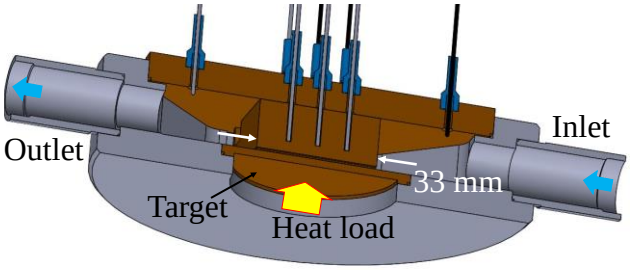

(a)

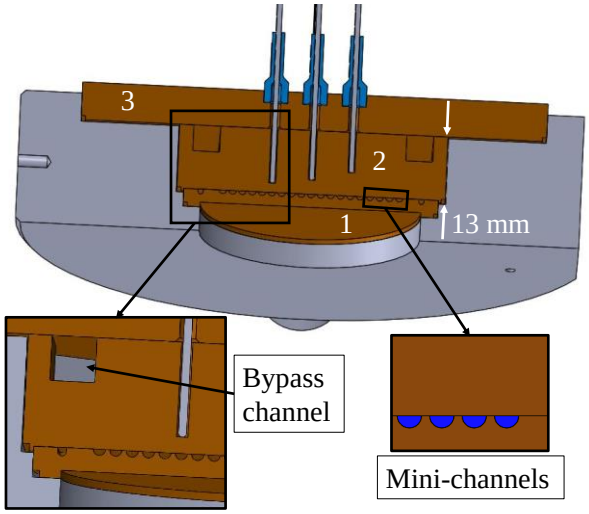

(b)

Fig. 2. CAD model of the cavity mock-up equipped with MC: (a) cut on the symmetry plane; (b) cut in a plane orthogonal to the MC. The various regions of the mock-up are also represented: (1) target region, (2) Glidcop block that closes the MC and includes the bypass channels, (3) copper lid of the mock-up. The inset on the left shows the detail of one of the two bypass channel. The inset on the right shows in blue the region in which the water flow is present (the flow direction is normal to the plane section).

II. THE MOCK-UP LAYOUT

The sections of the final version of the mock-up equipped with MCs are shown in Fig. 2. The central region of the structure is made of Glidcop® (CuAl15 [6]), a copper-aluminum alloy widely used in the gyrotron field, in which the set of MCs is drilled, while the external structure of the mock-up is made of copper. In the upper part of the central region, a set of thermocouples are also installed.

The mock-up structure is made by three different regions, see Fig. 2b, which are brazed together on their perimeter. Region 1 has a circular shape (~ 45 mm in diameter) and constitutes the so-called target, where the heat load is expected to be deposited on an area of 28 mm x 28 mm.

The hexahedral block above the MCs (region 2) is placed in contact with the block where the channels are drilled (region 1) and brazed externally on the copper structure. On the top of the structure in Fig. 2, a lid closes the part of the mock-up not exposed to the heat load and holds the thermocouples in place (region 3).

In total, 19 equal-spaced semi-circular MCs with diameter of 1.5 mm are drilled in region 1, ~ 2 mm apart from the heated surface. That distance is compatible with an actual design of mini-channels (MS) in the full-size gyrotron cavity, so that the cavity inner surface would still deform uniformly in the radial direction during steady state operation. The minimum channel-to-channel distance between any MCs is 0.5 mm. As Fig. 2b shows, the channels are positioned with the curved side exposed to the heated surface.

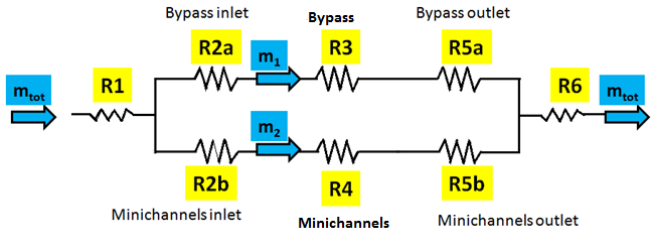

Fig. 3. Sketch of the simplified model for the evaluation of the pressure loss in the cavity mock-up equipped with mini-channels. The mass flow rate repartition is highlighted in light blue while the various hydraulic impedance are highlighted in yellow.

A. *Design of the bypass channels*

To mitigate the pressure drop across the mock-up and meet the facility pressure operation range, two identical 5.5 mm × 5.5 mm square bypass channels are drilled in the hexahedral region (see inset in Fig. 2b), at the two opposite bottom corners in region 2 (see Fig. 2b), in parallel with the MCs. The by-pass channels are sized in order to obtain hydraulic conditions (Reynolds number) similar to those in the full-size gyrotron at the nominal mass flow rate, see below, using the simplified pressure loss model reported in Fig. 3. Following the coolant direction: R1 gives the localized pressure loss due to the enlargement of the flow cross section from the mock-up inlet pipe to the mixing chamber upstream of the central block. R2a (R5a) and R2b (R5b) give the contributions of inlet (outlet) section of mini-channels and bypass pipe, R3 and R4 take into account the distributed pressure losses along the MCs and bypass channel, respectively, and R6 gives the localized pressure drop due to the reduction of cross section from the manifold downstream of the block to the mock-up outlet pipe. Since it is difficult to evaluate analytically the effect on the pressure drop due to the variation of flow area in the mock-up inlet and outlet, it has been evaluated numerically by means of a pure hydraulic simulation without any obstacle along the fluid path, see below for details.

The localized pressure loss at the MC and bypass inlet and outlet (R2a, R2b and R5a, R5b in Fig. 3) have been evaluated considering the variation of flow area from and to infinite regions by the correlation (1) [7]:

$$\Delta p_{R2+R5} = 1.4 \times \frac{G^2}{2\,\rho} \tag{1}$$

where: G [kg/(s m^2)] represents the specific mass flow rate in any channel, and ρ is the fluid density.

The distributed pressure loss inside MCs and bypass channels have been evaluated considering the correlation (2):

$$\Delta p_i = f_{R_i} \times \rho \, \frac{v^2}{2\,D_h} l \tag{2}$$

where: v is the fluid speed, D_h and l are the hydraulic diameter and the length of the channels, respectively; f_{R_i} is the friction factor of the different channel geometry, given in the semi-

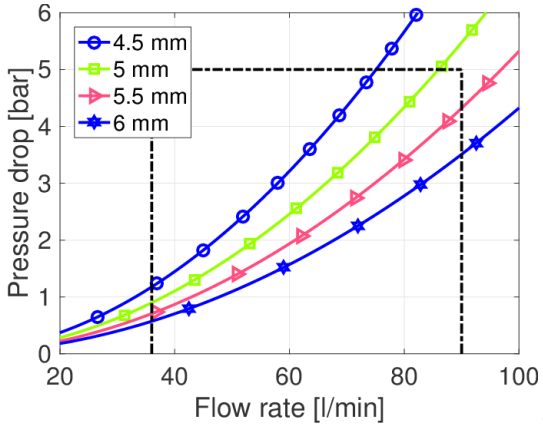

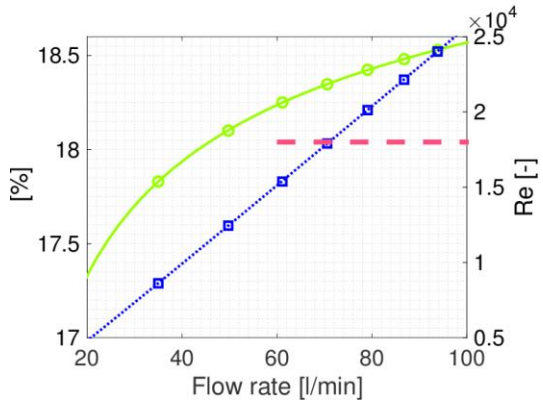

Fig. 4. (a) Pressure drop as a function of the flow rate computed with the simplified model of the cavity mock-up, for different dimension of the bypass channels (solid lines). The region included in the dashed rectangle highlights the operational range of the facility (b) Left axis: estimation of the fraction of the mass flow rate inside the MC (solid line with symbols) and right axis: comparison between mock-up (dotted line with symbols) and full size cavity (thick dashed line) average Re number inside the MC.

empirical correlations (3) and (4) for the rectangular and semi-circular channels, respectively.

$$f_{R3} = [0.79 \times \log(Re_C) - 1.64\,]^{-2} \quad (3)$$

$$f_{R4} = [-1.8 \times \log_{10}(6.9/Re)]^{-2} \times g(c) \quad (4)$$

Re_C in (3) is the Re number corrected with a function of the rectangle aspect ratio [8], and Re in (4) is the Reynolds number evaluated using the hydraulic diameter as characteristic length, while the function g(c) depends on the channel geometry. For the semicircular ducts in complete turbulent flow regime g(c) = 1, while for laminar conditions g(c) = c/64, where c is 63.017 [9].

Fig. 4a shows the characteristics curves obtained with different by-pass channel side dimension. The flow rate region between 36 l/min and 90 l/min, see below, and limited to 5 bar represents the working condition suitable for the test campaigns on gyrotron mock-up. The analytical results obtained shows that the 5.5 mm solution allows respecting the constraint of a maximum pressure drop of 5 bar imposed for the test campaign with the mass flow rate of 90 l/min [6].

The representativeness of the flow condition of the full-size cavity, in terms of Re number inside the MC, is guaranteed by the mass flow rate of 70 l/min in the mock-up test campaign

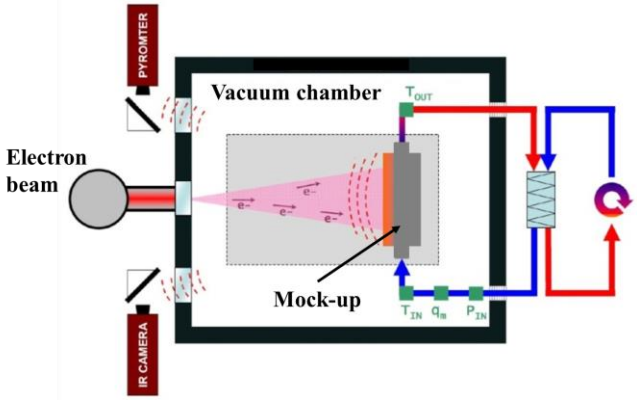

Fig. 5. Sketch of the FE200 test facility. The vacuum chamber (black thick line) together with the mock-up (dark grey), the electron beam (pink region) as well as the mock-up cooling circuit (red and blue arrows) are shown. Also the relevant diagnostic is represented (pyrometer and IR camera in red boxes, flow meters, pressure taps and temperature sensors in green boxes). (Adapted from [10])

(see Fig. 4b), with ~ 18% of the total mass flow rate flowing through the MC region.

III. Test Results

A. *Facility, diagnostics and operating conditions*

The experimental campaign on the cavity mock-up has been performed on December 1st, 2016 at the Areva NP Technical Centre of Le Creusot (France) in the FE200 test facility (see Fig. 5). The mock-up is placed inside a vacuum chamber with internal pressure maintained at 10^{-5} mbar. The mock-up is connected to the primary hydraulic loop in which the water flow could be adjusted between 0.6 kg/s (~ 36 l/min) and 6 kg/s (~ 360 l/min). The primary hydraulic loop can be regulated in temperature up to 230 °C and inlet pressure between 6 bar and

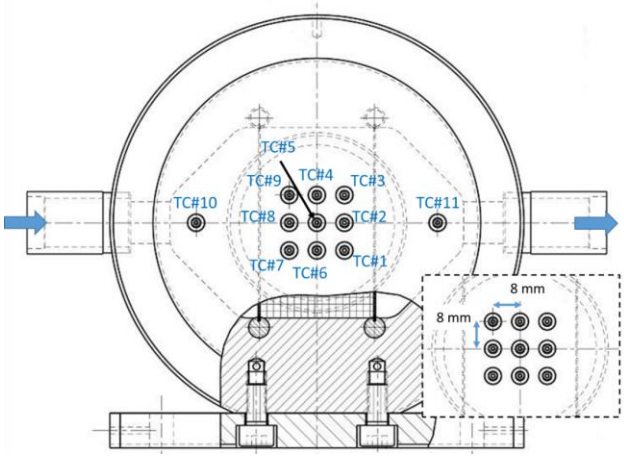

Fig. 6. Sketch of the thermocouples location in the mock-up (thermocouples numbered from #1 to #11). The inset shows the zoom of the region where the 9 thermocouples are positioned, together with their relative distance. The flow direction is also shown with the light blue arrows.

TABLE I
DISTANCE OF THE THERMOCOUPLES FROM THE HEATED TARGET SURFACE

Label	Distance from the heated surface
TC#1, TC#6, TC#7	4.75 mm
TC#2, TC#5, TC#8	5.75 mm
TC#3, TC#4, TC#9	7.75 mm

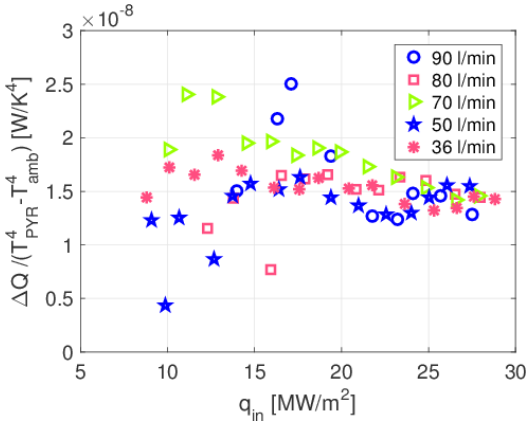

Fig. 7. Ratio between the experimental power losses (defined as $\Delta Q = Q_{gun} - Q_{in}$) and the difference between ambient and pyrometer temperatures to the fourth power as function of the heat load from calorimetry (q_{in}). The results available at various mass flow rates are represented (symbols).

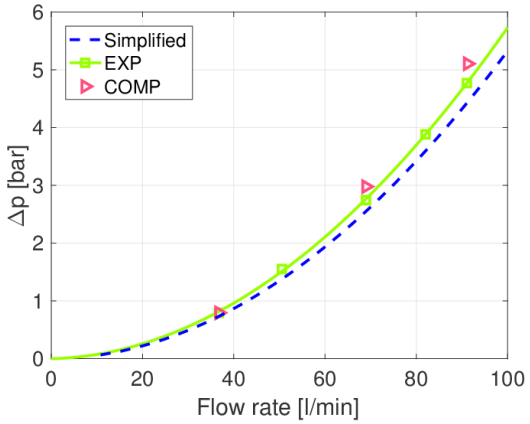

Fig. 8. Measured pressure drop across the mock-up, for the different tested flow rates (squares) and simulated flow rates (triangles). The quadratic fit of the experimental data (solid line), as well as the computed hydraulic characteristic (dashed line), are reported.

33 bar. A secondary loop is used to cool-down and to regulate the primary circuit. The coolant conditions of the primary coolant circuits are monitored by means of water mass and pressure meters at the mock-up inlet and two T-type thermocouples located before and after the mock-up [10].

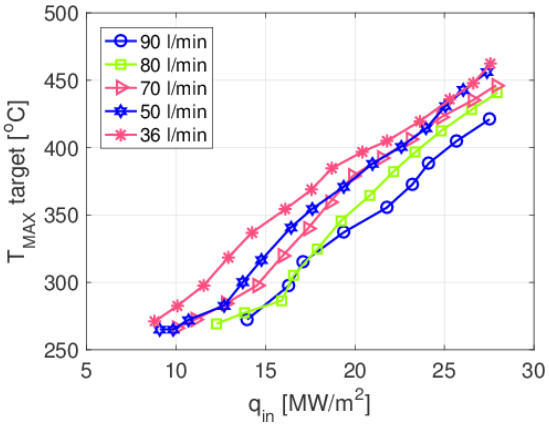

Fig. 9. Glidcop block bulk temperature measured by thermocouple TC#1 at the different tested mass flow rates as function of the heat load. (The position and the label of the thermocouples are described in Fig. 6).

The temperature measurement of the heated surface is provided by a pyrometer pointed on the target center and an infrared (IR) camera. While the data of the IR camera are not available due to issues in the data acquisition, the pyrometer has been calibrated in the range 265 °C – 455 °C [10], with an uncertainty lower than 0.2°C. The temperature inside the solid structure of the mock-up is measured by a set of 11 K-type thermocouples: 2 thermocouples are placed upstream and downstream the MCs region directly in the water stream, while the remaining 9 are positioned inside the Glidcop® hexahedral block. The position of the thermocouples and the distance with respect to the heated surface are shown in Fig. 6 and Table I, respectively. The error of the K-type thermocouples is considered equal to ± 1.5 °C.

Different water flow rates (nominally 36, 50, 70, 80 and 90 l/min) were tested during the measurement campaign, with an inlet pressure of 8.9 – 9.7 bar and an inlet temperature of 40 °C in all cases.

The target surface is heated by the electron gun on a 28 mm × 28 mm surface in the center of the target region. The heat entering the mock-up (Q_{in}) is computed by calorimetry from the power extracted by the coolant and q_{in} is the heat load computed by Q_{in} and the dimensions of the heated area. The difference with respect to the power in output from the electron gun (Q_{gun}) can be attributed to the radiative losses from the hot target surface, as it roughly scales with ($T_{surface}^4 - T_{ambient}^4$), see Fig. 7. The presence of radiative losses is peculiar of the planar geometry of the cavity mock-up: in the (final) cylindrical geometry of the gyrotron cavity, the hot surface is the inner side of the cavity itself, therefore the radiative losses are negligible.

B. Measurement results

The measured hydraulic characteristics of the mock-up at the Areva premises is reported in Fig.8, showing that the experiment results falls nicely around a quadratic fit in the mass flow rate, as expected. If, from one side, no information on the exact position of the pressure taps is available, although we know that the measured pressure drop should also include some minor pressure losses outside from the sample, on one other side the sensibility of the instrumentation is not available. The comparison with the pressure drop computed using the simplified analytical model, see above, gives a good agreement with an error lower than 10%.

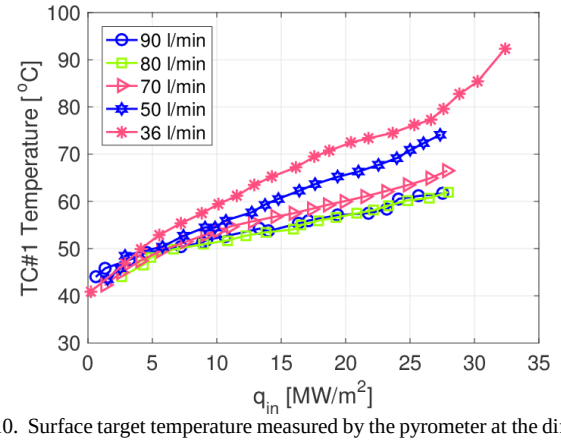

Fig. 10. Surface target temperature measured by the pyrometer at the different tested mass flow rates as function of the heat load.

The heated surface temperature measured by the pyrometer at the different heat loads computed from calorimetry (q_{in}), for the different flow rates, are displayed in Fig. 9. Inside the pyrometer calibration range, the trend of the signals shows an increasing temperature with the heat load for a given mass flow rate, and an increasing temperature for the same heat load when the mass flow rate decreases, as expected. The temperatures measured by the thermocouples show a similar trend, see the test results of TC#1 for instance in Fig. 10. However, the reconstruction of a 3D map of the temperature inside the Glidcop block is difficult in view of the uncertainty on the actual location of the junction of the thermocouples, so that we can look at trends of the same thermocouple but not compare directly the temperature measured by different thermocouples.

IV. Simulations

The simulations on the mock-up are performed with the commercial software STAR-CCM+ v. 11 [5].

A. Geometry

The geometry used in the simulations is shown in Fig. 2, with the only difference that the thermocouples are removed in the simulation computational domain. Symmetry of the geometry, boundary conditions for the solid domain and driver allow the simulation of just half of the mock-up.

B. Material properties

The temperature dependence of the material properties (density, thermal conductivity and specific heat) for Glidcop® and copper is taken into account in the simulations [11], [12].
The dependence on pressure and temperature of the liquid water properties is taken from [13], while the vapor properties are evaluated at the saturation temperature, corresponding to the pressure at the end of the MC region.

C. Boundary conditions

The simulated tests have been limited to three most relevant cases characterized by an inlet mass flow rate of 36 l/min, 70 l/min and 90 l/min, considering a 28 mm x 28 mm square shaped heat load applied to the heated zone of 5, 10, 12, 15, 18, 21, 24 and 27 MW/m^2 (note that we apply directly to the mock-up the heat load as resulting from the calorimetry on the sample, so that the modeling of the radiative losses can be neglected).

D. Model and simulation setup

The setting of the steady-state simulations is described here:

- 3D, steady state
- Turbulence model: k-ω SST [14], All y+ Wall Treatment
- Gravity: off.

The boiling model used is called in the software "Single Phase Boiling Model" [5], a very simple model which simulates the fluid as single phase and evaluates the heat load extracted by the boiling using the Rohsenow correlation (5) [5].

$$q_{bw} = \mu_l h_{lat} \sqrt{\frac{g(\rho_l - \rho_v)}{\sigma}} \left(\frac{Cp_l (T_w - T_{sat})}{C_{qw} h_{lat} Pr^{n_p}} \right)^{3.03} \quad (5)$$

where μ_l is the liquid dynamic viscosity, h_{lat} is the latent heat of vaporization, g is the gravitational acceleration, ρ_l and ρ_v are the liquid and vapour density, respectively, σ is the surface tension, Cp_l is the liquid heat capacity at constant pressure, $T_w - T_{sat} = \Delta T_{sat}$ is the difference between the wall temperature and the saturation temperature, C_{qw} is an empirical coefficient depending on the liquid-solid interface conditions (materials, surface conditions, …), and $Pr = \mu \frac{C_p}{k}$ is the Prandtl number with its exponent $n_p = 1$ [15]. The use of this model is justified by the low impact on the flow dynamics of the vapor bubbles generated at the MCs surfaces. The production of vapor is in fact expected to be low due to the high velocity inside the channels and the small area of the channels reached by high heat load >15 MW/m^2.
Due to the lack of information on the coefficient C_{qw} for the water-Glidcop® interface, the value 0.0147 (characteristic of the coupling water and lapped copper) is assumed [16].
Due to the presence of the contact interface between the block with the mini-channels (region 1 in Fig. 2b) and the hexahedral block above (region 2 in Fig. 2b), two set of simulations are performed modifying the value of the thermal contact resistance (Rc). In the first set of simulations the thermal resistance is considered zero, perfect contact between the two blocks; later the simulations are characterized by Rc = 1e-5 m^2 K/ W, which is inside the range of validity for copper-copper contact resistance [16].
The characteristics of the mesh used in all the simulations are defined in order to obtain inside the MCs region a value of wall y+ > 30 at the fluid-solid interface, as prescribed by the selected models, for any working conditions simulated, see the appendix A. Due to the very different flow conditions observed in the channels and in the other part of the structure, the wall y+ condition above is not satisfied everywhere, but the "All Wally+ Treatment" developed in the turbulent model adopted guarantees accurate results for any condition. The grid independence of the solution has been carefully checked.
As far as the simulation run is concerned, at any flow rate, steady-state pure hydraulic simulations are performed first, and then the heat load is switched on (segregated energy solver model) and increased step by step.

E. Comparison to the experimental results

The hydraulic characteristics, computed in absence of heat load, matches the experimental one (if we take seriously the data measured during the mock-up test campaign) within an accuracy of 10 %, see Fig. 8 (similar quality of agreement is found if the Realizable k-ε model [17] is used, not shown).
The computed mass flow rate distribution between the MCs and the by-pass channels is described in Table II, in which the average Reynolds number (Re) inside the MCs is also evaluated confirming the representativeness of the tests at the 70 l/min

TABLE II
Total inlet mass flow rate, computed mass flow rate in MCs and Re in the MC region.

Inlet mass flow rate	MC mass flow rate	Re
630 g/s (36 l/min)	110 g/s	0.9x10^4
1140 g/s (70 l/min)	210 g/s	1.7x10^4
1500 g/s (90 l/min)	280 g/s	2.3x10^4

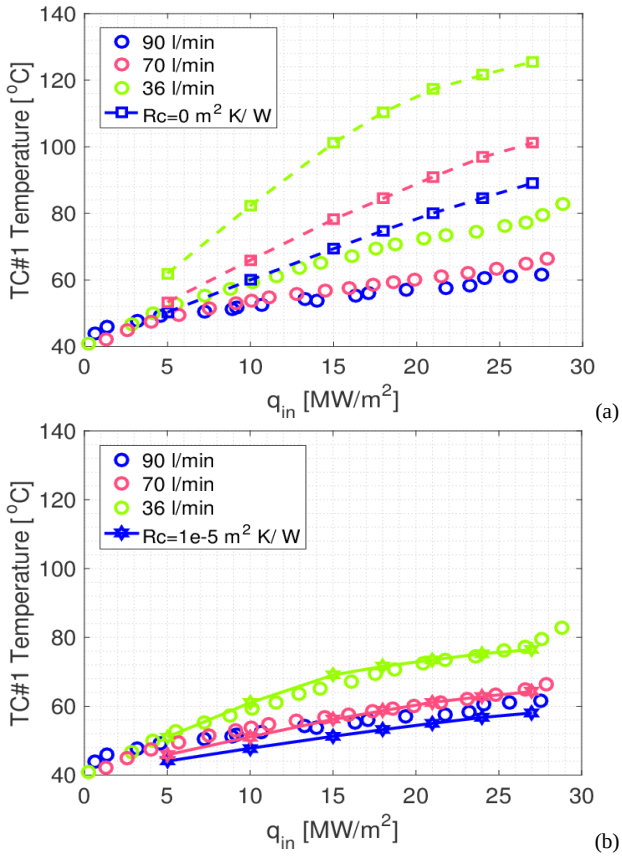

Fig. 12. Comparison between experimental (circles) and computed (lines) temperatures at the position of the TC#1 with Rc = 0 m^2W/K (a) and Rc = 1e-5 m^2W/K (b). The different colors correspond to the different tested mass flow rates.

flow rate for the full size cavity (where the design Re is ~ 1.8 x10^4) [18].

The main features of the experimental surface temperature are reproduced by the simulations at any flow rate and heat load, see Fig. 11, although the measured target temperature is systematically underestimated by the model by up to ~ 50 K (in the worst case, i.e. the case at the lowest flow rate), which corresponds to a relative error on the temperature increase up to ~ 20 %. The agreement improves when a finite contact resistance between the target and the hexahedral block is taken into account, see above, with a maximum relative error on the temperature increase below 15 %. That corresponds to a maximum error (over-estimation) on the maximum heat load handling capability up to ~ 20 % at 70 l/min. The effect of boiling in the simulations is shown by the variation of the slope of the curves toward the higher heat loads, that is more evident for lower mass flow rates which are characterized by wider boiling phenomena.

While the residual difference between computed and measured surface temperature remains unexplained, it is shown in Fig. 11 how it increases when the boiling phenomena are more pronounced. Should the new pressure drop measurement be confirmed, a lower fraction of the mass-flow rate in the mini-channels region than what is currently computed, would lead to a much better agreement in the evaluation of the target surface temperature, especially when the convective part of the heat transfer to the coolant is dominant on boiling (not shown). As far as the thermocouples are concerned, Fig. 12 shows the detailed comparison between the computed values and the experimental results neglecting or considering Rc. While the computed temperature without Rc largely disagree with the measured values, the effect of the inclusion of the contact resistance Rc in the model is quite remarkable: its value has been tuned on a single case (36 l/min and 24 MW/m^2) and then frozen. The error computed by the simulation at the different thermocouples, both in terms of absolute error and relative error at the highest heat load (27 MW/m^2), at the different flow rates is reported in Fig. 13. The relative error is computed as the difference between the experimental and the computed temperatures, divided by the difference between the experimental temperature and the inlet temperature of the coolant (40 °C). Considering the uncertainties of the experimental campaign [10] (e.g. exact location of the thermocouples measurement point, measurement uncertainties, data acquisition uncertainties), and the uncertainties of the simulations, we consider the

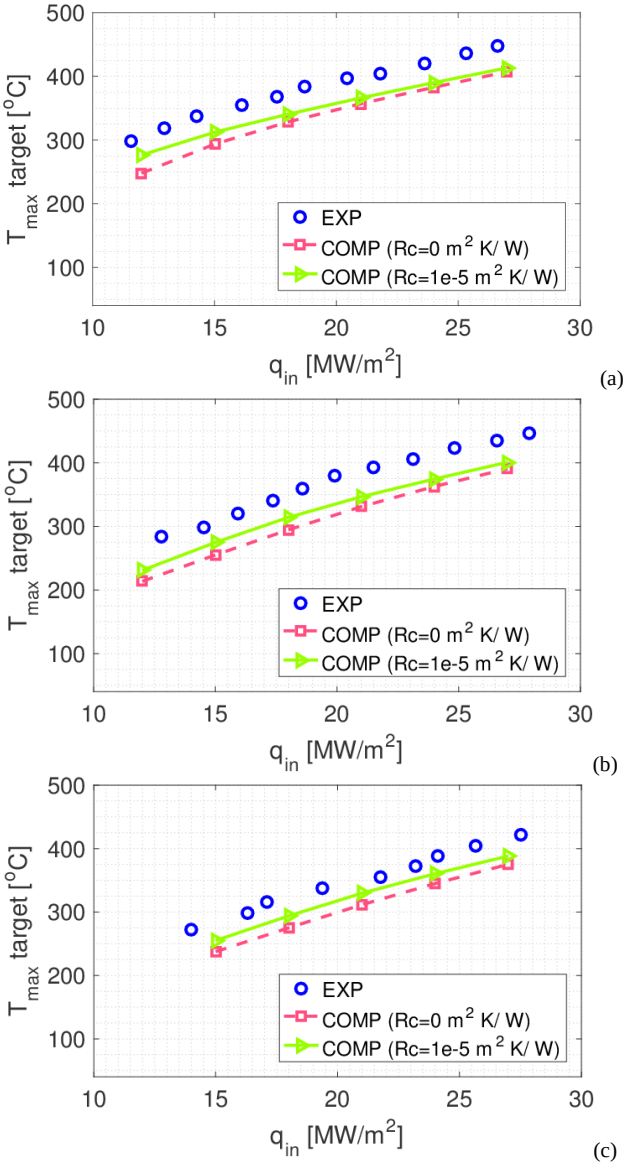

Fig. 11. Comparison between the pyrometers temperature (circles) and the computed maximum temperature on the heated surface (solid lines with triangles and squares), for a mass flow rate of: (a) 36 l/min, (b) 70 l/min and (c) 90 l/min, respectively, considering the two values of Rc employed in the analysis.

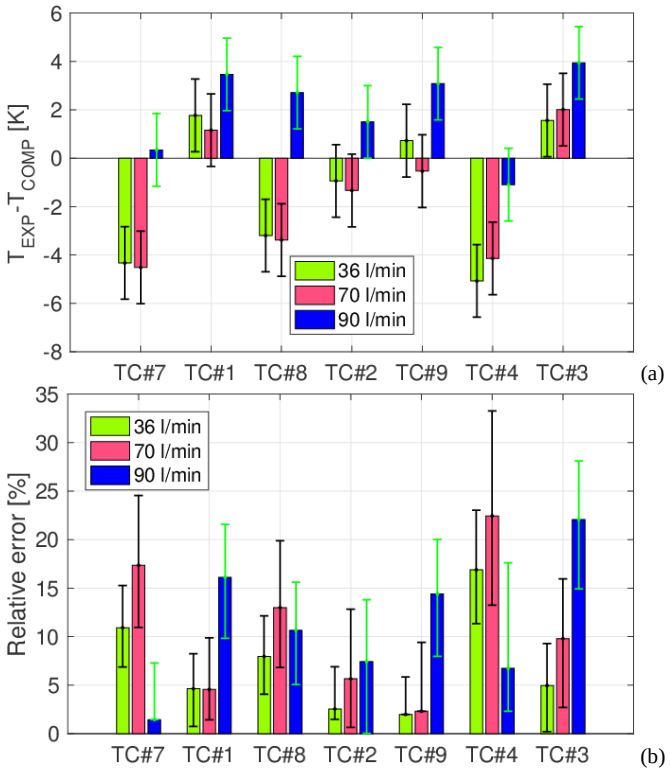

Fig. 13. Comparison between experimental and computed results in terms of (a) absolute and (b) relative error for working thermocouples, at the various tested mass flow rates and q_{in} = 27 MW/m^2. Errors are computed considering thermocouples accuracy of ±1.5 °C.

comparison between experimental and computed results to be satisfactory, with a maximum relative error lower than 22 % and maximum temperature difference lower than 5 °C.

Note that no comparison is meaningful on the TC#10 and TC#11, since the former just measures the inlet temperature, being upstream of the heated region, while the latter shows just a marginal temperature increase, while the former is in the mixing chamber downstream of the heated region, but located very far from the heated surface.

Summarizing, the relative difference between the measured and computed peak temperature increase on the target surface remains below 15% in the worst case, with an average relative error of 10%. The overall relative error on the temperature increase measured by the thermocouples inserted at different locations in the Glidcop block is on average below 10% as well.

The effect of a different turbulence model (Realizable k-ε [17]) on the computed results is negligible both in terms of maximum temperature on the heated surface and temperature on the thermocouples positions.

The relevant effect of the contact resistance, see also Fig. 14, is due to the different repartition of the heat load coming from heated surface. A parallel path is available to the heat flow: a conductive one through the solid teeth of the MCs in contact with the above-placed hexahedral block, in which the 9 thermocouples are positioned, and a convective one to the water boiling flow. In case of an additional contact resistance placed between the MCs and the hexahedral block above them, the conductive path is characterized by a higher thermal resistance, therefore less power reaches the block where the thermocouples are present and a lower temperature is detected in that region. On the other hand, more power goes to the fluid. Nevertheless,

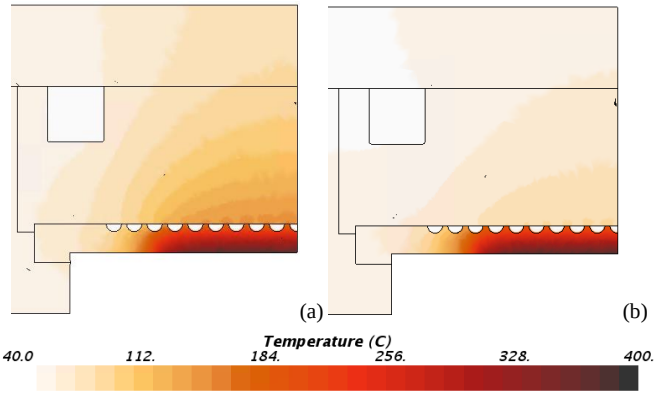

Fig. 14. Computed temperature maps (working conditions: 36 l/min, 24 MW/m^2) on a plane orthogonal to the mini-channels direction in the center of the target surface of the mock-up with. Rc equal to 0 m^{2}K/W (a) and 10-5 m^{2}K/W (b).

being the subcooled nucleate boiling very efficient in terms of heat transfer, the effect on the maximum surface temperature is not as relevant (> 50 °C) as the one on the thermocouples.

V. Conclusions and Perspective

A planar mock-up of the cavity of the European 170 GHz, 1 MW gyrotron for ITER has been designed with a set of semi-circular mini channels (diameter = 1.5 mm) to remove the heat load impacting on the Glidcop® target, and with a couple of square by-pass channels (5.5 mm side) to allow the flow conditions in the MC regions to be representative of those in the full-size cavity.

The experimental results confirm the pressure losses as evaluated by a simplified analytical model used for the preliminary design procedure, and by CFD, giving and indirect confirmation also of the estimated mass flow repartition between the MCs and the bypass channels.

The mock-up showed that a heat load of ~ 21 MW/m^2 can be removed by the forced flow of highly sub-cooled pressurized water in a set of mini-channels, while still keeping the maximum surface temperature below 400 °C (in flow conditions representative of the full-size cavity). The mock-up was also successfully exposed to a heat load of 27 MW/m^2 reaching ~ 450 °C at the lowest mass flow rate.

The test results were also used to calibrate and validate a CFD model of the system based on the commercial software STARCCM+, with particular attention to the choice of the turbulence and boiling models and to the effect of the contact thermal resistance Rc between the Glidcop® target and the bulk the structure of the mock-up.

In perspective, the good agreement between simulations and measurements (within 15 % for the surface temperature increase, or 20 % for the maximum heat load which the device can handle at the mass–flow rate relevant for the full-size cavity) shows that the model can be considered a reliable tool for the thermal-analysis of a full-size gyrotron cavity equipped with mini-channels.

Acknowledgements

A. Bertinetti should like to thank Areva for kind hospitality during the tests. We thank F. Cimolin (CD-adapco support) for useful discussions on the implementation of the models in

STARCCM+. L. Savoldi acknowledges the financial support of F4E through the Expert Contract F4E-2015-EXP-223.

REFERENCES

[1] M. Henderson, G. Saibene, C. Darbos, D. Farina, L. Figini, M. Gagliardi, et al., "The targeted heating and current drive applications for the ITER electron cyclotron system", Phys. Plasmas, vol. 22, 021808, 2015.

[2] F. Albajar et al., Status of Europe's contribution to the ITER EC system, EC-18, Nara, Japan, Apr. 22-25, 2014, EPJ Web of Conferences 87 (2015) 04004.

[3] J. M. Coulson and J. F. Richardson, *Chemical Engineering Desing*, 4th ed., vol. 6, USA: Elsevier, 2005.

[4] L. Savoldi, A. Bertinetti, G.F. Nallo, A. Zappatore, R. Zanino, F. Cau, F. Cismondi and Y. Rozier, "CFD Analysis of Different Cooling Options for a Gyrotron Cavity", *IEEE Trans. Plasma Sci.*, vol. 44, no. 12, pp 3432-3438, Nov. 2016.

[5] Star-CCM+ User's Manual v11.04.

[6] Y. Rozier, private comunication, August 2015.

[7] F. M. White, *Fluid mechanics*, 7th ed., New York, USA: McGraw-Hill, 2009.

[8] O. C. Jones jr., "An improvement in the calculation of turbulent friction in rectangular ducts", *J. Fluid Eng.*, vol. 98, *no.* 2, pp. 173–181, June, 1976.

[9] S. Kakac, R. K. Shah and W. Aung, *Handbook of Single-Phase Convective Heat Transfer*, USA: John Wiley & Sons, 1987.

[10] A. Leggieri, Report on thermal cavity mock-up experiments, F4E_D_27P69S v1.0, April 2017.

[11] J.W. Davis, P.D. Smith, "ITER material properties handbook", Journal of Nuclear Materials, vol. 233-237, no. 2, pp. 1593 -1596, Oct. 1996.

[12] http://www-ferp.ucsd.edu/LIB/PROPS/PANOS/cu.html, accessed on April 2017.

[13] http://www.iapws.org, accessed on April 2017.

[14] F.R. Menter, "Two-equation eddy-viscosity turbulence modeling for engineering applications", *AIAA Journal*, vol. 32, no. 8, pp. 1598-1605, 1994.

[15] J. G. Collier, *Convective Boling and Condensation*, 3rd ed., Oxford Science Publications, Clarendon Press, 1994.

[16] F.P. Incropera, *Introduction to heat transfer*, 6th ed., USA: John Wiley & Sons, 2011.

[17] T.-H. Shih, W.W. Liou, A. Shabbir, Z. Yang, and J. Zhu, "A New k-ε Eddy Viscosity Model for High Reynolds Number Turbulent Flows -- Model Development and Validation", NASA TM 106721, 1994.

[18] A. Bertinetti, K. A. Avramidis, F. Albajar, F. Cau, F. Cismondi, Y. Rozier, L. Savoldi, R. Zanino, "Multi-physics analysis of a 1 MW gyrotron cavity cooled by mini-channels", *Fus. Eng. Des., vol. 123, pp. 313-316, Nov.* 2017.

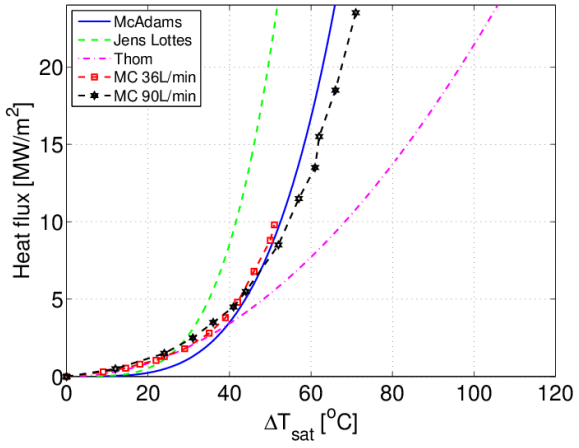

Fig. 15. Comparison of the typical subcooled nucleate boiling correlations (solid, dashed and dash-dotted lines) with the results obtained varying the mass flow rate of the CFD simulations (dashed lines with symbols).

VI. APPENDIX A: VALIDATION OF THE BOILING MODEL

The boiling model adopted in the simulations (see above) has been validated in a controlled case study against correlations available in literature [15]. The case study consists in a uniformly heated pipe, long enough to guarantee fully developed thermal and hydraulic profiles. The heat flux has been imposed as driver of the simulations computing as output the wall temperature.

The comparison, see Fig. 15, has been performed in terms of heat flux vs. ΔT_{sat}, defined as $\Delta T_{sat}=T_w-T_{sat}$.

Different quantitative trends are obtained using the correlations and this is explained by the fact that they have been obtained from different sets of experimental results [15]. On the other hand, as expected, the computed results with different values of the mass flow rate show the very same behavior, since in presence of subcooled boiling the inlet velocity as well as the initial sub-cooling do not affect the heat transfer performance. Further, it can be observed that if boiling is not present, the heat transfer capability are much more downgraded with respect to those with the boiling enabled. Note that the single phase boiling model needs a mesh with $y+ > 30$ in order to correctly switch on the Rohsenow correlation [5].

Finally, the comparison of the correlations with the computed results shows a good agreement both at low fluxes with the Thom correlation as well as at high fluxes with the McAdams one. The single phase boiling model is therefore able to reproduce correctly the heat transfer enhancement due to subcooled nucleate boiling.

Andrea Bertinetti received the B.Sc. in Energy Engineering in 2013 and M.Sc. degrees in Energy and Nuclear Engineering in 2015 from the Politecnico di Torino, Turin, Italy.
He is currently a Ph.D. student at Politecnico di Torino since 2015.
His present activities involve the CFD analyses of the ITER gyrotron cavity and the preliminary modeling of DEMO pressure suppression system.

Ferran Albajar received the master's degree in Industrial Engineering in 1997 and the PhD in nuclear engineering in 2001 from the Polytechnic University of Catalonia. He was a researcher at the Commissariat à l'Energie Atomique (Cadarache), at the University of Pavia (Pavia) and at the Polytechnic University of Catalonia (Barcelona) contributing to the modelling of the energy transport in fusion plasmas. He worked in industry on renewable energy systems and civil engineering. He joined F4E in 2008, and since 2011 he is a Senior Technical Officer on the ITER heating systems.

Alberto Leggieri received the M.Sc. degree and Ph.D in electronic engineering in 2011 and 2016 respectively from University of Rome "Tor Vergata". From 2011 to 2017 he was with S.I.T. S.p.A as R&D engineer and radiofrequency laboratory manager where he was involved in the design of medical particle accelerators. From 2017 he is with THALES Electron Devices as hyperfrequency development engineer, where he is involved in the design of gyrotron oscillators for nuclear fusion. His research interests are in the development of vacuum tubes, LINAC and spatial power combiners. He serves as a referee for several journals, among which IEEE Transactions on Microwave Theory and Techniques and Progress in Electromagnetic Research.

François Legrand received the university diploma in physical measurements with the specialization in nuclear measurements in 1991 from University of Paris "UPSUD". From 1994 to 2011 he has studied several disciplines as cryogenics and vacuum science (University of Orsay), fluid mechanics (INSA-Lyon) and radiofrequency electronics (IUT Ville d'Avray). He started working in 1991 with Thomson Tubes Electroniques and he followed the company until the evolution in THALES Electron Devices, where he actually works as vacuum tube product specialist. During more than 25 years, he developed the industrial design of several gyrotron oscillators for various fusion machines among which the W7-X Stellarator and ITER Tokamak. His research interests are in the development of vacuum tubes, ultra high vacuum systems and nuclear fusion facilities.

Etienne Perial received the Master's degree in engineering and management and the Master in Business Administration (MBA) in 2001 and 2002 respectively. From 2002 to 2012 he was with Renault, formerly as industrial process designer and then as manufacturing facility manager. From 2012 he is with THALES Electron Devices, formerly as manufacturing process head of travelling wave tube and actually as program manager of scientific products. Currently, he is involved in the manufacturing process management and installation of gyrotron oscillators for nuclear fusion purposes.

Francesca Cau graduated in electrical engineering in 2003 at the University of Cagliari (Italy) and received the PhD in industrial engineering in 2007.
From 2007 to 2010 she worked at CRPP Villigen (Switzerland) in the frame of a program financed by the European Commission and focused on Magnet Technology for Fusion (MATEFU).
She has been working in F4E since 2010 where she is responsible mainly for thermo-hydraulic analyses. She is author of more than 50 publications, most of them related to ITER.

Laura Savoldi (M'11) received the M.Sc. degree in nuclear engineering and the Ph.D. degree in Energetics from Politecnico di Torino (PoliTo), Italy. She has been Professor of nuclear engineering at Dipartimento Energia, PoliTo, since 2017. Her research interests are in the development, validation, and application of computational tools for the analysis of thermal-hydraulic transients in super-conducting magnets, and in this frame, she developed the 4C code for the analysis of thermal-hydraulic transients in superconducting cables, coils and related cryogenic circuits. She co-authored 120+ papers published in international journals and proceedings of international conferences. Prof. Savoldi serves as a referee for several international journals and conferences of her field of

research, among which IEEE Transactions on Applied Superconductivity and IEEE Transactions on Plasma Science.

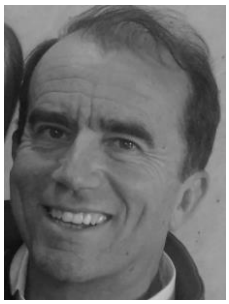

Roberto Zanino (M'11–SM'13) received the M.Sc. degree in nuclear engineering and the Ph.D. degree in energetics from Politecnico di Torino (PoliTo), Italy.

Since 2000, he has been a Professor of nuclear engineering at Dipartimento Energia and since 2011 he is the Head of the graduate studies in Energetics, both at PoliTo. He is the author or coauthor of 150+ papers that appeared in international journals devoted to the computational modeling in fields of relevance for nuclear fusion (superconducting magnets and cryogenics, plasma-wall interactions, high heat flux components, ...), nuclear fission (Gen-IV lead-cooled fast reactors) and concentrated solar power (central tower system receivers). Prof. Zanino is a member of the American Nuclear Society and regularly serves as a referee for the IEEE Transactions on Applied Superconductivity.

Andrea Zappatore received the B.S. and M.S degrees in energy and nuclear engineering in 2014 and 2016, respectively. He has been undergraduate researcher since 2013 with the Energy Department, Politecnico di Torino, under the guidance of Prof. Zanino and Savoldi, contributing to various works on the modeling of components for nuclear fusion applications, such as High Temperature Superconducting (HTS) current leads (CL) and superconducting magnets and the Computational Fluid Dynamics analysis of fusion devices components. He has been enrolled in the Ph.D program in Energetics in 2017.